Journal of Nuclear Materials 400 (2010) 232–239

Contents lists available at ScienceDirect

Journal of Nuclear Materials

journal homepage: www.elsevier.com/locate/jnucmat

Nickel solubility limit in liquid lead–bismuth eutectic

L. Martinelli [a,*], F. Vanneroy [a], J.C. Diaz Rosado [b], D. L'Hermite [b], M. Tabarant [b]

[a] CEA, DEN, DPC, SCCME, Laboratoire d'Etude de la Corrosion Non Aqueuse, F-91191 Gif-sur-Yvette, France
[b] CEA, DEN, DPC, SCP, Service de Chimie Physique, F-91191 Gif-sur-Yvette, France

ARTICLE INFO

Article history:
Received 12 March 2009
Accepted 17 March 2010

ABSTRACT

In the framework of the Accelerator-Driven System (ADS), the Pb–Bi eutectic can be used as spallation target for neutron production. The Pb–Bi flow in contact with the ADS structural steels, T 91 (Fe–9Cr martensitic steel) and 316L (Fe–17Cr–10Ni austenitic steel), can dissolve the main steel components: iron, chromium and nickel. According to literature, in low oxygen containing Pb–Bi, the dissolution rates of 316L depend, at least, on the nickel solubility limit as it dissolves preferentially in the Pb–Bi alloy. Consequently, the determination of this physico-chemical data in the temperature range of the ADS operating conditions (350–450 °C) is needed for the prediction of the corrosion rates in ADS.

The nickel solubility limit in Pb–Bi is available in the literature from 400 °C to 900 °C but not for lower temperatures. However, the Ni–Bi phase diagram leads one to suppose that the nickel solubility limit law changes for lower temperatures. Consequently in this study, two experimental techniques have been implemented for the determination of the nickel solubility limit at low temperatures. The first one is performed from 400 °C to 500 °C using the Laser Induce Breakdown Spectroscopy (LIBS). The LIBS technique permits to obtain in situ measurements directly performed on liquid Pb–Bi. This characteristic is very interesting as it allows to monitor on line the concentration of the dissolved impurities in the liquid coolant. However, this technique is still under development and optimization on liquid Pb–Bi medium. The second technique is ICP-AES. This technique, commonly used to analyze alloys composition, is interesting as it permits a global analysis of a Pb–Bi sample. Moreover, the measurement made by ICP-AES is very reliable, very accurate and optimized for such analyses. However, this technique is ex situ; this is its main disadvantage. Experiments using ICP-AES were performed from 350 °C to 535 °C. The two techniques lead to the same solubility limit in their common temperature range. However, the experiment using ICP-AES technique revealed a change in the nickel solubility law for the temperatures lower than 415 °C. Consequently, this study recommends the use of two solubility limits relations, which take into account these results, as well as the literature results: the solubility limits laws of Martynov and Rosenblatt. The nickel solubility limit can thus be expressed as: $\mathrm{Log}\ S_{\mathrm{Ni}}(\mathrm{wt.\%}) = 5.2 \pm 0.12 - \frac{3500}{T(\mathrm{K})}$ for the temperature range: 330–415 °C. This law is the empirical solubility law obtained in this study at the low temperature range. $\mathrm{Log}\ S_{\mathrm{Ni}}(\mathrm{wt.\%}) = 1.7 \pm 0.08 - \frac{1009}{T(\mathrm{K})}$ for 415–900 °C temperature range. This law is the linear regression made on the overall experimental points available in literature and in this study. According to the Martynov studies, it seems reliable up to 900 °C.

1. Introduction

This study takes place in the framework of the feasibility studies of the Accelerator-Driven Systems (ADS) reactors. These reactors are a technical option for transmuting long-lived nuclear wastes. In such systems, lead–bismuth eutectic (45 wt.%Pb–55 wt.%Bi) is considered to produce, through a spallation process, the large excess of neutrons needed to sustain the nuclear reaction in the subcritical blanket. The Pb–Bi eutectic (LBE) appears to be a good candidate, due to its high atomic number, low melting point (125 °C), fast heat removal from the target, good neutron yield and low vapour pressure. However, liquid metals can be corrosive towards containment materials: mainly austenitic steel 316L (Fe–17Cr–10Ni) and martensitic steel T 91 (Fe–9Cr–1Mo). The prediction of corrosion kinetics of 316L by the liquid LBE requires the determination of the solubility limits of the main material elements in the LBE. Values of solubility limits of iron, chromium and nickel are available in the literature for a temperature range equal to 400–900 °C for the nickel and the chromium and 550–980 °C for iron. Previous studies, on 316L corrosion in LBE, showed that nickel, which solubility limit is higher than that of iron and chromium, preferentially dissolved in LBE [1]. Consequently, the knowledge of the solubility limit values for nickel seems essential.

* Corresponding author. Address: CEA-Saclay, DEN/DPC/SCCME/LECNA, Bât. 458 Point courrier n° 50, 91191 Gif sur Yvette Cedex, France. Tel.: +33 1 69 08 16 13; fax: +33 1 69 08 15 86.
E-mail address: laure.martinelli@cea.fr (L. Martinelli).

0022-3115/$ - see front matter © 2010 Elsevier B.V. All rights reserved.
doi:10.1016/j.jnucmat.2010.03.008

As the ADS operating temperatures are between 300 °C and 450 °C, the accurate determination of the nickel solubility limit in this temperature range is needed.

The main objective of this study is to measure the nickel solubility limit as a function of temperature between 300 °C and 550 °C. The proposed temperature range is chosen according to the double interest to:

(i) obtain an empirical nickel solubility limit in LBE for temperatures corresponding to the normal operating conditions and to some operational transients;
(ii) compare the obtained solubility limit relation to the literature data given for temperatures higher than 400 °C.

In this study, two experiments are performed to measure the nickel solubility limit in LBE as a function of temperature. The first one is performed using ex situ analysis on LBE samples removed at regular time intervals. The nickel analysis is obtained with ICP-AES which is a very accurate measurement. Its lower detection limit is equal to 30 ppb. The second one is performed by Laser Induced Breakdown Spectroscopy (LIBS). Its lower detection limit is higher than the ICP-AES one but the main interest of this technique is the performance of in situ measurements.

The goal of this double experiment is firstly to obtain the nickel solubility limit for the whole temperature range of the ADS operating conditions; and secondly to evaluate the interest of the LIBS technique for in situ measurements in Pb–Bi coolant. This last point is promising for nuclear industry. Indeed, the in situ impurities concentration measurement can be an indirect measurement of structural steel corrosion rate in reactor. For instance, if the 316L dissolution becomes important in the reactor, nickel is released in the Pb–Bi coolant. Consequently the nickel concentration evolvement in the coolant gives information about the 316L corrosion level. One in situ measurement of nickel (and iron, chromium for other steels) concentration by week would thus permit to check the good performance of 316L (and other structural steels) in the reactor. This experiment is moreover the first LIBS measurement performed on a lead–bismuth alloy to our knowledge.

Firstly, literature data on solubility limits of the main metallic impurities are given. The experiment methodology and the two analytical techniques are then detailed. In the last part of this study the results are presented and discussed.

2. Literature review

The solubility limits of the main metallic elements in pure lead, in the Pb–Bi eutectic (LBE) alloy and in pure bismuth, given by the literature are gathered in Table 1. Usually, the solubility limit of a metallic element X in the liquid metal is obtained by the dissolution in the liquid metal of a X metallic sample.

Liquid metal samples are removed at regular time intervals and the concentration of the element X is measured by atomic absorption spectroscopy. The solubility limit is considered to be reached when the concentration of the element X is stabilized [2].

For metallic elements with high solubility limits, the X metallic sample is immersed in the liquid metal and removed at regular time intervals. The sample weight loss is measured as a function of time. The solubility limit is obtained when the weight loss does not evolve any longer [3].

The solubility limits of iron, chromium and nickel in LBE are presented in Fig. 1 as a function of temperature.

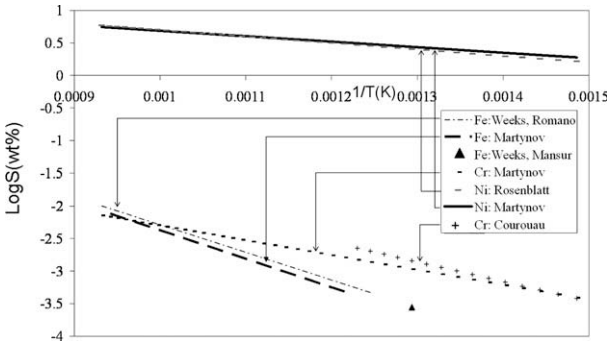

Fig. 1. Solubility limits of iron, chromium and nickel in liquid Pb–Bi.

Table 1
Fe, Cr, Ni solubility limits in Pb, Bi and Pb–Bi eutectic.

Element	Solubility limits (wt.%)		
	Pb	LBE	Bi
Fe	$\mathrm{Log}(S) = 0.34 - \frac{3450}{T}$ $395 < T < 600$ °C $\mathrm{Log}(S) = 1.824 - \frac{4860}{T}$ $600 < T < 750$ °C [8] $\mathrm{Log}(S) = 2.53 - \frac{5314}{T}$ $750 < T < 1300$ °C [12]	$\mathrm{Log}(S) = 1.96 - \frac{4246}{T}$ $525 < T < 840$ °C Pb-52, 6%Bi [8] $\mathrm{Log}(S) = 2.01 - \frac{4380}{T}$ $550 < T < 780$ °C [4] $\mathrm{Log}(S) = -3.55$ (500 °C) [6]	$Log(S) = 1.832 - \frac{3589}{T}$ $440 < T < 725$ °C [6]
Cr	$\mathrm{Log}(S) = 3.7 - \frac{6720}{T}$ [10] $\mathrm{Log}(S) = 3.74 - \frac{6750}{T}$ $908 < T < 1210$ °C [8]	$\mathrm{Log}(S) = -0.02 - \frac{2280}{T}$ $400 < T < 500$ °C [5] $\mathrm{Log}(S) = 1.07 - \frac{3022}{T}$ $370 < T < 540$ °C [11]	$\mathrm{Log}(S) = 2.5 - \frac{3717}{T}$ $390 < T < 725$ °C [6]
Ni	$\mathrm{Log}(S) = 1.3 - \frac{1383}{T}$ $613 < T < 1073$ °C [9] $\mathrm{Log}(S) = 2.78 - \frac{1000}{T}$ $603 < T < 1573$ °C [17] $\mathrm{Log}(S) = 3.75 - \frac{2189}{T}$ $773 < T < 1073$ °C [7]	$\mathrm{Log}(S) = 1.7 - \frac{1000}{T}$ $480 < T < 550$ °C [5] but linear regression on experimental points coming from [5] leads to: $\mathrm{Log}(S) = 1.65 - \frac{960}{T}$ $Log(S) = 1.53 - \frac{843}{T}$ $400 < T < 900$ °C [4] $\mathrm{Log}(S) = 1.6 - \frac{920}{T}$ 415 °C $< T < 535$ °C (this study) $\mathrm{Log}(S) = 5.2 - \frac{3500}{T}$ 350 °C $< T < 415$ °C (this study)	$\mathrm{Log}(S) = 2.61 - \frac{1538}{T}$ $450 < T < 630$ [6] $\mathrm{Log}(S) = 0.458 - \frac{616}{T}$ $755 < T < 1283$ [7]

Fig. 1 shows that, for each metallic element (Fe, Cr, Ni), the different solubility laws are in good agreement.

The solubility limits of iron and chromium are close. However, for temperatures lower than 660 °C, the iron solubility limits are slightly lower than the chromium solubility limits except for the pure lead medium [10] (see Table 1). The solubility limits of nickel are about 300 times higher than the solubility limits of iron and chromium. For iron and chromium, the solubility limits in Pb–Bi eutectic are lower than the ones in pure bismuth and higher than the ones in pure lead. Important discrepancies exist in the literature results for the solubility limit of Nickel in pure lead and in pure bismuth (see e.g. Figs. 2, 3). In pure bismuth, the nickel solubility given by Weeks [6] is more than eight times higher than the one given by Nash [7] (Fig. 3). In pure lead, the nickel solubility given by Nash [7] is more than 25 times higher than the one of given by Alden [9] (Fig. 3). However, the two solubility laws [4,5] in LBE are very close. Fig. 3 emphasizes the great discrepancy of the solubility limit values in pure lead and in pure bismuth: it shows that, depending on the chosen solubility law, the nickel is either more soluble in pure lead than in pure bismuth or the contrary. The phase diagrams of Ni–Bi (Fig. 4) and Ni–Pb (Fig. 5) show a higher solubility of nickel in pure bismuth than in pure lead. To settle this issue, other experiments are needed. However, one can assume that the nickel solubility limit in pure bismuth is higher than the one in pure lead: (i) as bismuth is always more reactive than lead (see solubility limits of iron and chromium, Fig. 1) and (ii) as a more important affinity between Ni and Bi is revealed by the presence of intermetallic compounds Ni–Bi (see diagram Fig. 4). Finally, the solubility limit of nickel in LBE has been measured in the temperature range 400 °C to 900 °C whereas the temperature range of the ADS operating conditions is between 350 °C and 450 °C. An extrapolation of the Martynov's [4] and the Rosenblatt's [5] laws could be made to the lower temperatures to evaluate the nickel solubility limit at 350 °C, but the Ni–Bi phase diagram presented in Fig. 4 shows that the Ni–Bi solid phase, $NiBi_3$, is formed for temperatures lower than 469 °C. The presence of this intermetallic phase changes the nickel solubility limit in pure bismuth, as the dissolved nickel, in equilibrium with solid NiBi at higher temperature ([5], Fig. 4), becomes in equilibrium with $NiBi_3$. No Ni–Bi–Pb phase diagram exists in the literature but a similar Ni–Bi(Pb) phase is able to appear at low temperatures in LBE. The Martynov's law, which is obtained for temperatures between 400 °C and 900 °C, does not present any change. Therefore, according to the Martynov's law, only one solid phase exists in equilibrium with the dissolved nickel in LBE from 400 °C to 900 °C.

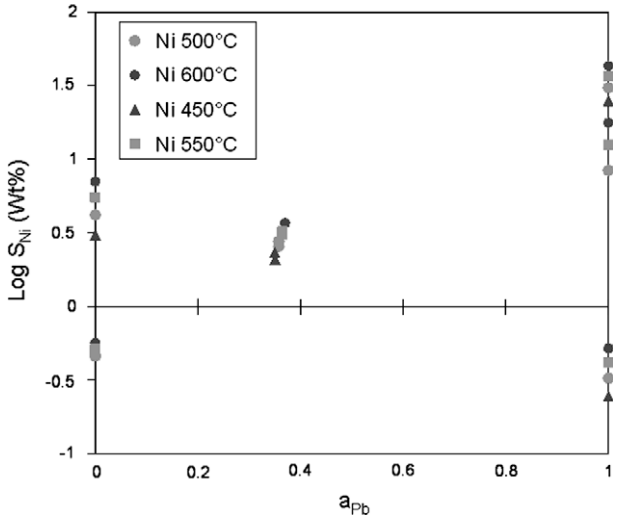

Fig. 2. Solubility limits of iron and nickel as a function of lead activity in the Pb–Bi alloy at 550 °C.

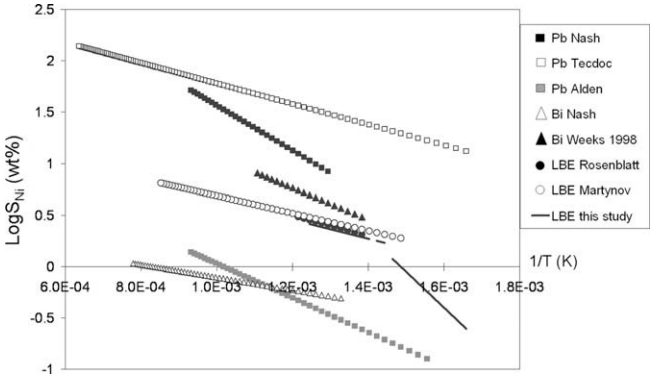

Fig. 3. Solubility limits of nickel in pure lead, LBE and pure bismuth as a function of the temperature inverse.

The purpose of this study is thus, firstly, to determine the nickel solubility limit at low temperatures. Secondly, it is to verify if different solid phases appear in chemical equilibrium with the dissolved nickel in the temperature range of the ADS operating conditions. In this study, the nickel solubility limit will be obtained with two different experimental facilities in order to obtain, firstly, a reliable solubility limit for nickel and secondly to test an in situ analysis technique, which seems promising for in situ measurements of impurities in LBE.

3. Experimental

3.1. Experiment principle

The principle of the Ni solubility limit measurement is to dissolve a Ni sheet in oxygen purified Pb–Bi eutectic at a given temperature T_1.

A measurement of the Ni concentration is carried out at regular time intervals using either ICP-AES or LIBS analyses.

(i) In the case of ICP-AES analysis, a LBE sample is removed for measurement of the Ni concentration. The methodology of this measurement is summarized in Section 3.3.
(ii) In the case of LIBS analysis, a laser beam impacts the liquid LBE surface through a window leading to the Ni concentration analysis (see Section 3.4).

When at T_1, the Ni concentration evolution becomes negligible, the Ni solubility limit is assumed as reached. The temperature T_1 is then decreased or increased (both are performed to evaluate the reliability of the measurement) at temperature T_2. After a while, thermodynamics equilibrium is established:

(i) in the case of temperature increase ("increasing temperature ramp" experiment), the Ni sheet dissolves until its concentration in LBE reaches its solubility limit and the Ni concentration in the LBE bulk is analyzed;
(ii) in case of a temperature decrease ("decreasing temperature ramp" experiment), the excess Ni precipitates at the LBE surface and the Ni concentration in the LBE bulk is analyzed.

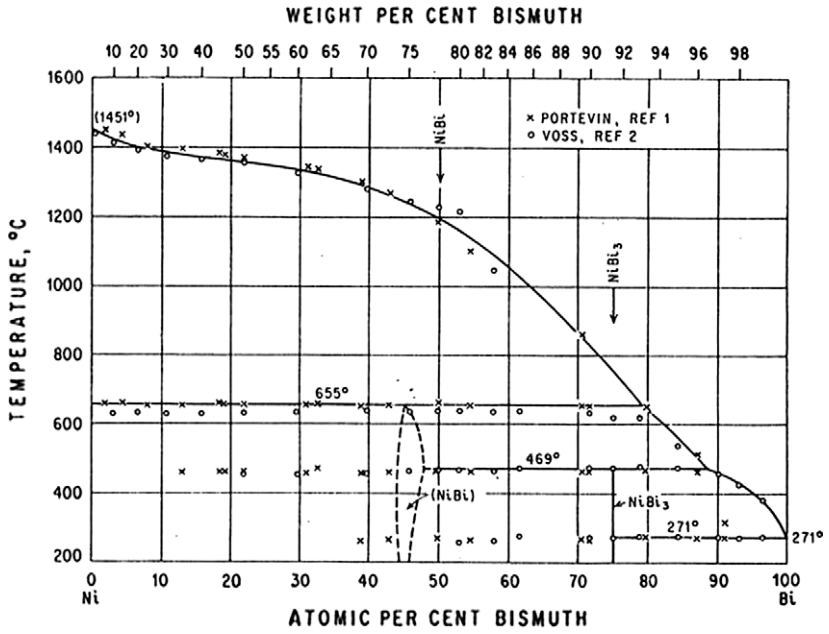

Fig. 4. Phase diagram of Ni–Bi [13].

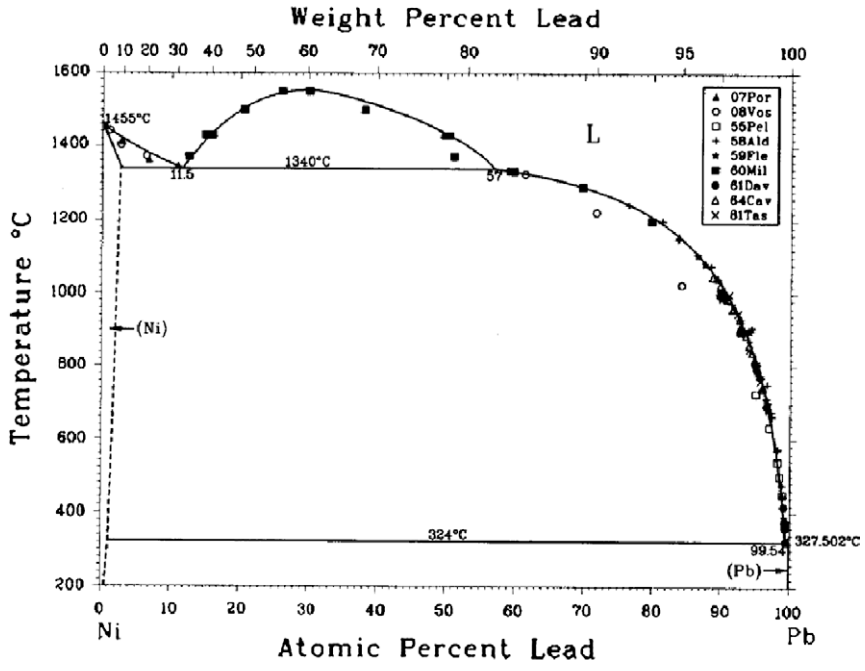

Fig. 5. Phase diagram of Ni–Pb [14].

When the concentration measurement is carried out via the LIBS analysis, only the LBE surface is analyzed. Consequently, only the increase of temperature ("increasing temperature ramp" experiment) is carried out for this experiment. When the Ni concentration does not evolve any longer, the Ni solubility limit is reached at the temperature T_2. The temperature is then in/decreased at the temperature T_3 and the experiment is repeated.

3.2. Experimental conditions

The nickel sheet sample is mirror polished and cleaned with ethanol before the experiments. The oxygen concentration is continuously measured in the LBE crucible to ensure that the formation of NiO is avoided. The oxygen measurement is performed by a specific oxygen sensor made of yttria stabilised zirconia (supplied by Umicore) [2,11]. The purification of LBE is obtained by a continuous Ar–4%H_2 sweeping. The temperature is measured by a thermocouple K immersed in LBE. To avoid the LBE pollution by the dissolution of the thermocouple 316L coating, the thermocouple K is inserted inside a Pyrex thimble before immersion in LBE. The temperature measurement must be very accurate in this study. To homogenise the temperature between both inside and outside of the thimble, it is filled with LBE, which is a good thermal conductor, ensuring a reliable temperature measurement.

Table 2
Characteristics of ICP operating conditions.

Plasma viewing	Number of measurements	Integration time (s)	Plasma power (W)	Coolant gas flow, (L min^{-1})	Auxiliary gas flow, (L min^{-1})	Nebulizer gas flow (L min^{-1})	Nebulizer
Axial	8	5	1300	15	0.8	0.7	Micro mist (glass expansion)

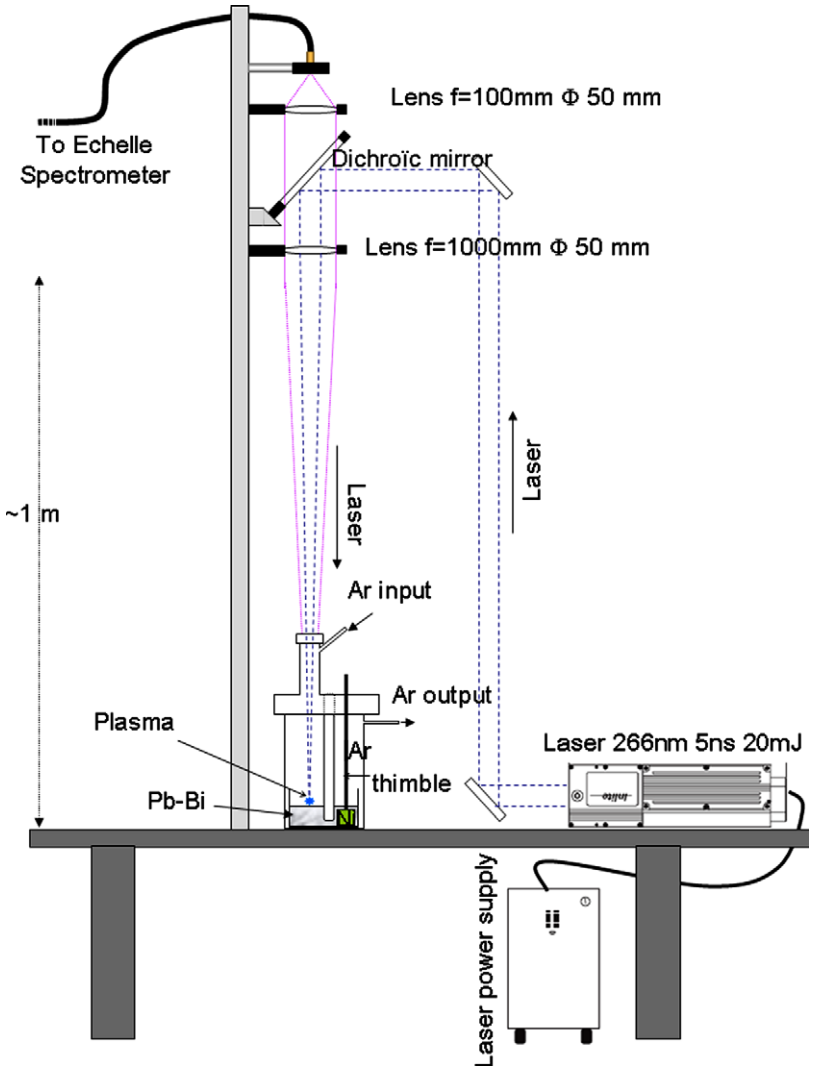

Fig. 6. Experimental facility for Ni solubility measurement using the LIBS measurement.

According to this protocol, the nickel solubility limit is obtained:

(i) for 11 different temperatures (from 330 to 535 °C) using the ICP-AES measurement technique (four temperatures during the "increasing temperature ramp" experiment and seven temperatures during the "decreasing temperature ramp" experiment);
(ii) and for three temperatures (from 397 to 460 °C) using the LIBS technique.

These results are presented in Fig. 7.

3.3. Experiment with ICP-AES analyses

One of the main interests of the ICP-AES technique is to allow a global analysis of the removed LBE sample. It means that the ICP-AES technique can analyze a sufficiently important LBE volume to be considered as representative of the global bulk chemistry. Consequently, the volumes of the removed LBE samples are between 0.25 and 0.5 cm^3.

The ICP-AES analysis goes off into two stages. The first stage consists in the LBE sample dissolution in order to obtain an ICP-AES analysable solution. This solution has been optimized to measure very small quantities of metallic impurities in LBE leading to an accuracy of 1.5%.

The whole LBE sample is weighed and placed in a PFA vessel. To dissolve the sample, 10 ml of nitric acid (analytical grade, 15 M), per gram of LBE, and 10 ml of oxygen peroxide (analytical grade), per gram of LBE, are added. The mixture is warmed at approximately 80 °C during 3 h.

After digestion, the volume is adjusted to 50 ml with a solution of nitric acid (0.5 M). This solution, containing the dissolved LBE

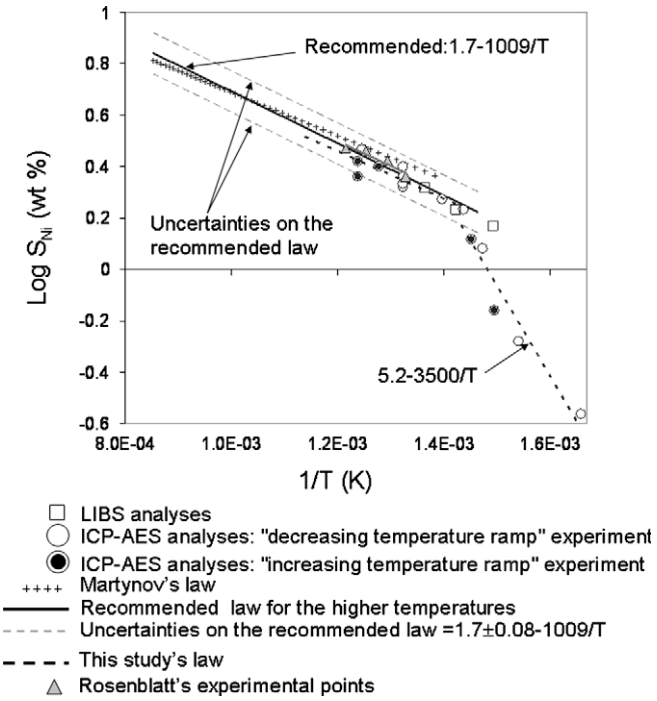

Fig. 7. Results of Ni solubility limits obtained in this study with the two analyses techniques. Comparison with literature data.

sample, is then analyzed. Knowing the Ni solubility limit, these dilutions lead to a concentration in Ni equals to about 0.1–1 μg per millilitre.

The second stage consists in the determination of the dissolved Ni concentration in the previously obtained solution. This measurement is performed using elementary analysis with induced coupled-plasma atomic emission spectroscopy (ICP-AES, Perkin Elmer Optima 2000DV). Three wavelengths are used to validate the method (231.604 nm, 221.648 nm and 232.003 nm). Six standard solutions of Ni (SPEX Plasma Standards) at concentrations between 0.1 and 1 wt. ppm are analyzed to obtain a calibration curve for each wavelength.

This curve was used to calculate the concentration of Ni in the solution and then in the LBE sample.

The characteristics of the ICP operating conditions are gathered in Table 2.

3.4. Experiment with LIBS analyses

The Laser Induced Breakdown spectroscopy (LIBS) is an analytical technique based on the measurement of the emitted light from a plasma produced by an intense pulsed laser beam [15,16].

The setup (Fig. 6) consists of two subsystems: a laser with an optical focusing system, and a collecting system with a spectrometer to analyze the light emitted by the plasma. The Inlite II Nd:YAG frequency-quadrupled laser (Excel Technology) delivers 266 nm wavelength pulses with a 5 ns pulse width and a 20 mJ pulse energy at 20 Hz repetition rate. The 6 mm diameter beam is transported by mirrors and deviated into the furnace by a dichroic beam splitter that reflects the laser wavelength (226 nm) and transmits light at wavelengths exceeding 300 nm. The laser beam is then focused by a lens with a 1-m focal length. The laser penetrates into the furnace via a viewport that also ensures confinement. The energy deposited on the target at the focal point, in only a few nanoseconds, creates a plasma with the same composition as the material to be analyzed. The very high temperature of the plasma, consisting of atoms, ions, and electrons, emits light. This light is collected through the viewport, the focusing lens and the dichroic beam splitter. The focusing lens in this direction is used to collimate the light into a parallel beam. A second lens above the beam splitter injects light from the plasma into a 500 μm optical fiber leading to a spectrometer. The LLA echelle spectrometer is capable of simultaneously observing a wavelength range from 200 to 900 nm with a spectral resolution of 13,000 ($\lambda/\Delta\lambda$).

The measurement has been done as follows. The detection is temporally resolved using an Intensify Charged-Couple Device (ICCD). Delay and gate have been optimized to maximize signal to background ratio. The bests set of parameters are 700 ns for the delay and 2 μs for the gate. The gain of the ICCD is set to 3400 corresponding to an electronic amplification of 10^3. Each spectrum corresponds to an accumulation of 40 laser shots. Each measurement is a mean of four replicates. The intensity of the nickel spectrum is proportional to the concentration of nickel in LBE. Consequently, the calibration of the nickel spectrum is obtained by LIBS analysis on a LBE sample containing a known nickel concentration.

4. Results and discussion

The nickel solubility limit is reached, whatever the temperature, after maximum 24 h of Ni sheet immersion. Fig. 7 gathers the literature solubility limits and the solubility limit results (in wt.%) obtained in this study using the LIBS technique and the ICP-AES technique. The solubility limit obtained at the lowest temperature (330 °C) corresponds to the "decreasing temperature ramp" experiment. As the temperature is decreasing during the "decreasing temperature ramp" experiment, some metallic particles precipitate at the LBE surface. These precipitates are in thermodynamical equilibrium with the dissolved nickel at the test temperature (330 °C for the last temperature). The X-ray diffraction spectrum of these precipitates is presented in Fig. 8. It reveals the presence of the $NiBi_3$ intermetallic phase.

Fig. 7 leads to emphasize five characteristics of the results:

(i) There is agreement between both measurements, obtained by LIBS and by ICP-AES. This agreement shows that the obtained solubility limits are reliable and that they neither depend on the kind of experiment ("increasing temperature ramp" or "decreasing temperature ramp"), nor on the measurement technique (LIBS or ICP-AES).

(ii) Moreover, this agreement shows that the LIBS technique can be used to measure dissolved species in LBE, even if other experiments are needed to validate the technique in other conditions and to optimize the process. Indeed, to validate the technique, LIBS measurement should be performed in a Pb–Bi loop, with Pb–Bi in circulation. Moreover LIBS measurements could be also carried out in Pb–Bi containing solid oxides or metallic precipitates in order to evaluate if the measurement of dissolved species is disturbed by the presence of these solid particles. The process should also be optimized in terms of limit of detection. Indeed, this study shows that the dissolved nickel concentration can be measured by LIBS in Pb–Bi. However, as the nickel solubility limit is much higher than the one of iron or chromium, the limit of detection of the LIBS technique must be decreased in order to allow the measurement of the iron or the chromium concentration in Pb–Bi. The improvement of the limit of detection can be reached: (a) using a more luminous spectrometer; (b) improving the optical elements in order to increase the photon collection efficiency and to decrease

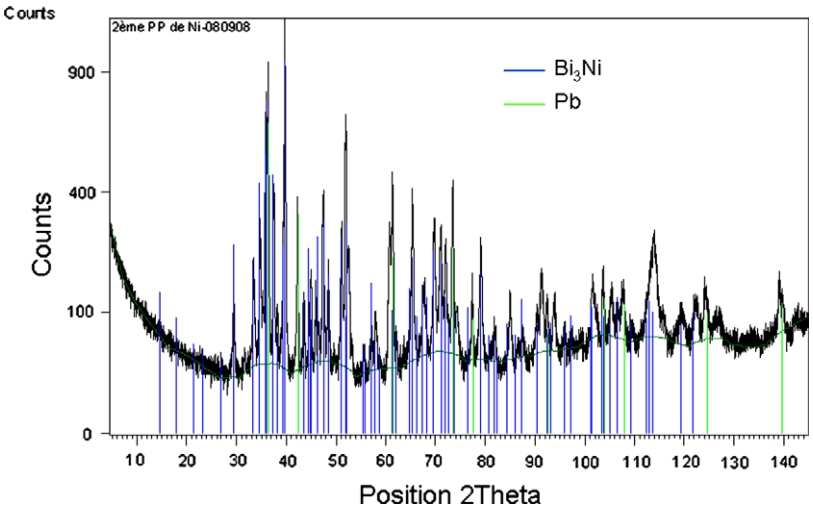

Fig. 8. X-ray diffraction of the precipitates removed from the LBE at the experiment end.

the spherical aberration and improving again the photon collection efficiency of the system; (c) reducing the distance between the liquid surface and the closest lens.

(iii) The solubility limit results are consistent: the solubility limit decreases when the temperature decreases. The solubility limits, obtained at a given temperature, are reproducible with a discrepancy equals to about 6.5%. The results obtained during the "increasing temperature ramp" experiment and during the "decreasing temperature ramp" experiment are in agreement: the dissolution/precipitation reversibility is validated. The solubility limits follow an Arrhenius law: $S_{Ni} = S_0 \exp\left(-\frac{E_A}{T}\right)$ (with E_A, the activation energy, S_{Ni}, the nickel solubility limit, S_0, the pre-exponential factor, T, the temperature). The experimental nickel solubility limit law is obtained by linear regression on experimental points.

(iv) Two solubility limits laws are obtained.

$$\text{Log } S_{Ni}(\text{wt.}\%) = 1.6 - \frac{920}{T(\text{K})} \quad (1)$$

for the 415–535 °C temperature range (see Fig. 7);

$$\text{Log } S_{Ni}(\text{wt.}\%) = 5.2 - \frac{3500}{T(\text{K})} \quad (2)$$

for the 330–415 °C temperature range (see Fig. 7). The transition between the two solubility laws is observed at about 415 °C.

(v) The solubility limit law, obtained for the highest temperatures, is in agreement with the literature data [4,5] for the same temperature range. Indeed, the results given by Martynov [4] are obtained for the 400–900 °C temperature range and the ones of Rosenblatt [5] are obtained between 480 and 550 °C.

The solubility limit law, obtained for the lowest temperatures, leads to lower solubility limit values than the calculated ones using the Rosenblatt's, or the Martynov's laws.

The reasons of the change of slope for the experimental nickel solubility law (Fig. 7) must be elucidated. It could be explained by kinetics reasons if the equilibrium is not reached but in that case, the nickel concentration would be higher than the calculated one with literature's laws. The change of slope in the solubility limit law could then be due to the precipitation of a different solid when the saturation level is reached. This different solid has been identified by X-ray diffraction at the end of the "decreasing temperature ramp" experiment: it is the $NiBi_3$ phase (see Fig. 8).

For the higher temperatures three solubility laws are thus available:

$$Log(S, \text{wt.}\%) = 1.53 - \frac{843}{T} \text{ for } 400 < T < 900\ ^\circ\text{C} \quad (3)$$

is given by the Martynov's studies [4]

$$\text{Log}(S, \text{wt.}\%) = 1.7 - \frac{1000}{T} \text{ for } 480 < T < 550\ ^\circ\text{C} \quad (4)$$

is given by the Rosenblatt's paper [5] but a linear regression on the experimental points coming from Rosenblatt's studies [5] (see Fig. 7) leads to:

$$\text{Log}(S, \text{wt.}\%) = 1.65 - \frac{960}{T} \quad (5)$$

$\text{Log}(S, \text{wt.}\%) = 1.6 - \frac{920}{T}$ for 415 °C < T < 535 °C is given by this study.

Fig. 7 shows that the various solubility laws are close. Moreover, the discrepancy in the experimental points seems to be in the same order of magnitude that the difference between the solubility laws. To quantify these differences, the following calculation is made for each experimental point and each solubility law.

$d = 100\frac{|S^T_{exp} - S^T_{Xlaw}|}{S^T_{Xlaw}}$ with d, the relative difference in %, S^T_{exp} the experimental solubility limit at the temperature T, and S^T_{Xlaw} the solubility limit obtained using the X's law (X = Robertson, Martinov, this study, recommended law) at the temperature T.

The results of the above calculation are summarized in Table 3. Table 3 shows that the most important relative difference d between experimental points and their own linear regression is given for the results obtained at low temperature in this study: 23%. The maximum difference between this study experimental points and the solubility laws is 25%: with the Martinov's law (against 21% with the Robertson's law and 14% with this study's law). Moreover approximately the same relative difference, d, exists between the solubility law given by (Eq. (1)) and the experimental results derived from this study at high temperature (14%) and between the solubility law given by (Eq. (1)) and the experimental results derived from Rosenblatt's study [5] (13%). It shows that the discrepancy in the obtained results is not insignificant. Considering this discrepancy, the three laws for the higher temperatures (higher than 415 °C) can be considered as the same laws.

Table 3
Maximum difference of solubility limit (in%) between experimental results and the various solubility laws.

High temperatures	Martinov's law [4] (Eq. (3))	Linear regression on Rosenblatt's experimental points [5] (Eq. (5))	This study's law (Eq. (1))	Recommended law (Eq. (6))
This study experimental points	25	21	14	17
Rosenblatt's experimental points [5]	11	3	13	9
Low temperatures			This study's law (Eq. (2))	
This study experimental points			23	

As the experimental points coming from the Martinov's study [4] are not available, a linear regression of the Rosenblatt's and this study's (for $T > 415$ °C) experimental points corresponds to a good approximation of the nickel solubility limit between 415 °C and 550 °C:

$$\text{Log } S_{Ni}(\text{wt.}\%) = 1.7 - \frac{1009}{T(\text{K})} \quad (6)$$

Fig. 7 shows that the values of the linear regression from the overall experimental points for temperature higher than 415 °C (Eq. (6)) gets closer to the Martinov's law when temperature increases. The relative difference, d, between the Martinov's law and that of (Eq. (6)) is 5% at 900 °C, less than 1% at 750 °C and 7% at 600 °C. As these relative differences are lower than that obtained with experimental points, it can be considered that the (Eq. (6)) is also a good approximation of the nickel solubility limit up to 900 °C.

Consequently, the (Eq. (6)), with a 17% uncertainty (maximum relative difference obtained between experimental points and the values from (Eq. (6)), see Table 3), is considered as a good approximation of the nickel solubility limit between 415 °C and 900 °C:

$$\text{Log } S_{Ni}(\text{wt.}\%) = 1.7 \pm 0.08 - \frac{1009}{T(\text{K})}$$

for 415–900 °C temperature range. In the considered range of temperature, this law is almost superposed on the Rosenblatt's law and the results obtained in this study and it also agrees very well with the Martinov's law for 450–900 °C temperature range (Fig. 7).

For the lower temperatures, the literature does not propose any law of nickel solubility limit. The one of this study is thus the only one. Considering a 25% uncertainty, it leads to:

$$\text{Log } S_{Ni}(\text{wt.}\%) = 5.2 \pm 0.12 - \frac{3500}{T(\text{K})} \quad (7)$$

for the 330–415 °C temperature range. The nickel solubility limit law is then now reliable from 330 °C to 900 °C.

5. Conclusions

The aim of this work was: (i) firstly, to obtain the nickel solubility limit in the temperature range of the ADS operating conditions (300–550 °C); (ii) secondly, to evaluate the interest of the LIBS in situ measurement in LBE coolant.

The obtained nickel solubility limits are:

$$\text{Log } S_{Ni}(\text{wt.}\%) = 5.2 \pm 0.15 - \frac{3500}{T(\text{K})}$$

for the 330–415 °C temperature range

$$\text{Log } S_{Ni}(\text{wt.}\%) = 1.6 - \frac{920}{T(\text{K})}$$

for the 415–535 °C temperature range. The solubility limit empirical relation for the higher temperature range is very close to the literature solubility limits coming from Martynov [4] (obtained from 400 °C to 900 °C) and Rosenblatt [5] (obtained from 480 °C to 550 °C). According to this study discussion, a solubility law derived from a linear regression of the overall available experimental points is recommended to be used from 415 °C to 900 °C:

$$\text{Log } S_{Ni}(\text{wt.}\%) = 1.7 \pm 0.08 - \frac{1009}{T(\text{K})}$$

for 415–900 °C temperature range. The nickel solubility limit proposed in this study for the lowest temperature range (330–415 °C) is then:

$$\text{Log } S_{Ni}(\text{wt.}\%) = 5.2 \pm 0.12 - \frac{3500}{T(\text{K})}.$$

Finally, this study emphasizes the interest of the LIBS technique use to obtain in situ measurement in LBE. Optimization of the technique should be performed in order to measure other metallic impurities inside LBE.

Acknowledgements

Authors thank the European project EUROTRANS for the contribution to the financing of this work. Authors thank K. Ginestar and H. Badji for their support for experiments and Dr D. You for his advice.

References

[1] Ph. Deloffre, A. Terlain, F. Barbier, J. Nucl. Mater. 301 (2002) 35–39.
[2] Handbook on Lead–Bismuth Eutectic Alloy and Lead Properties, Materials Compatibility, Thermal-Hydraulics and Technologies, OECD, Nucl. Sci., 2007, p. 129 (Chapter 4).
[3] N. Simon, T. Flament, A. Terlain, C. Deslouis, Int. J. Heat Mass Transf. 38 (16) (1995) 3085–3090.
[4] P.N. Martynov, K.D. Ivanov, in: Proceedings of Four Technical Meeting Held Between December 1995 and April 1998, 1998, pp. 177–184.
[5] G. Rosenblatt, J.R. Wilson, in: Proceeding of the Session IV on Corrosion by Liquid Metals of the 1969 Fall Meeting of the Metallurgical Society of AIME, Philadelphia, Pensylvania, 1969, pp. 469–477.
[6] J.R. Weeks, Materials for Spallation Neutron Sources, in: M.S. Wechsler, L.K. Mansur, C.L. Snead, W.F. Sommer (Eds.), The Minerals, Metals & Materials Society, 1998.
[7] P. Nash, Bull. Alloy Phase Diagr. 6 (1985) 345–347.
[8] J.R. Weeks, A.J. Romano, Corros. NACE 25 (3) (1969) 131–136.
[9] T. Alden, D.A. Stevenson, J. Wulff, Trans. Metall. Soc. AIME (1958) 15–17.
[10] M. Venkatraman, J.P. Neumann, Bull. Alloy Phase Diagr. 9 (1988) 155–157.
[11] J.L. Courouau, J. Nucl. Mater. 335 (2) (2004) 254–259.
[12] D.A. Stevenson, J. Wulff, Trans. Metall. Soc. AIME 221 (1961) 271–275.
[13] Hansen, Constitution of Binary Alloys, Metallurgy and Metallurgical Engineering Series, McGraw-Hill Book Company, INC., 1958.
[14] P. Nash, Bull. Alloy Phase Diagr. 8 (1987) 264–268.
[15] D. Cremers, L. Radziemsky (Eds.), Handbook of Laser-Induced Breakdown Spectroscopy, John Wiley & Sons, L0074d., 2006.
[16] A.W. Miziolek, V. Palleschi, I. Schechter (Eds.), Laser-Induced Breakdown Spectroscopy, Cambridge University Press.
[17] TECDOC-1289, Comparative Assessment of Thermophysical and Thermohydraulic Characteristics of Lead, Lead–Bismuth, and Sodium Coolants for Fast Reactors, IAEA, 2002.